

# Train at Moving Edge: Online-Verified Prompt Selection for Efficient RL Training of Large Reasoning Model

Jiahao Wu<sup>\*1,2</sup> Ning Lu<sup>\*1,3</sup> Shengcai Liu<sup>1</sup> Kun Wang<sup>4,2</sup> Yanting Yang<sup>5</sup> Qing Li<sup>2</sup> Ke Tang<sup>1</sup>

## Abstract

Reinforcement learning (RL) has become essential for post-training large language models (LLMs) in reasoning tasks. While scaling rollouts can stabilize training and enhance performance, the computational overhead is a critical issue. In algorithms like GRPO, multiple rollouts per prompt incur prohibitive costs, as a large portion of prompts provide negligible gradients and are thus of low utility. To address this problem, we investigate how to select high-utility prompts before the rollout phase. Our experimental analysis reveals that sample utility is non-uniform and evolving: the strongest learning signals concentrate at the “learning edge”, the intersection of intermediate difficulty and high uncertainty, which shifts as training proceeds. Motivated by this, we propose HIVE (History-Informed and online-VERified prompt selection), a dual-stage framework for data-efficient RL. HIVE utilizes historical reward trajectories for coarse selection and employs prompt entropy as a real-time proxy to prune instances with stale utility. By evaluating HIVE across multiple math reasoning benchmarks and models, we show that HIVE yields significant rollout efficiency without compromising performance.

## 1. Introduction

Reinforcement Learning (RL) has emerged as a prevalent paradigm for fine-tuning large language models (LLMs), particularly for enhancing complex reasoning capabilities (Guo et al., 2025; Yu et al., 2025; Jaech et al., 2024). Advanced RL algorithms such as group relative policy op-

<sup>\*</sup>Equal contribution <sup>1</sup>Southern University of Science and Technology, Shenzhen, China <sup>2</sup>The Hong Kong Polytechnic University, Hong Kong, China <sup>3</sup>The Hong Kong University of Science and Technology, Hong Kong, China <sup>4</sup>Nanyang Technological University, Singapore <sup>5</sup>Rutgers University, New Jersey, USA. Correspondence to: Shengcai Liu <liusc3@sustech.edu.cn>.

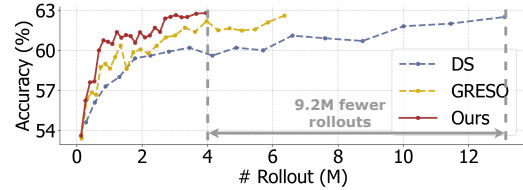


Figure 1. **Selection efficiency on five math reasoning benchmarks.** Using Qwen2.5-Math-7B trained on DAPO+MATH, we evaluate our approach (HIVE) against advanced baselines Dynamic Sampling (DS) and GRESO. HIVE exhibits superior efficiency, achieving comparable accuracy to DS while reducing up to 9.2M rollouts, also outperforming GRESO by a large margin.

timization (GRPO) (Shao et al., 2024) leverage verifiable rewards to refine model reasoning abilities through extensive rollouts during each training iteration. While increasing the number of responses sampled per prompt, known as rollout scaling, effectively stabilizes training and enhances model performance (Xu et al., 2025; Yu et al., 2025), it introduces a severe computational overhead. In the RL-based training of LLMs, the majority of computational resources are spent on generating rollouts for low-utility prompts that are either too trivial or too intractable for the current model. This results in vanishing gradients and wasted resources, providing no informative learning signal for model updates (Zheng et al., 2025b; Yu et al., 2025; Noukhovitch et al., 2025; Sheng et al., 2025a). Consequently, we investigate the following research question in this paper: *How to select valuable prompts for more efficient rollout scaling?*

Existing methods for prompt selection in RL-based fine-tuning face limitations. Traditional static methods rely on predefined heuristics (Wang et al., 2025b; Li et al., 2025b; Ye et al., 2025b), failing to capture evolving utility across models and training stages. To address this, recent online methods (Xu et al., 2025; Chen et al., 2025a; Ye et al., 2025a), such as Dynamic Sampling (Yu et al., 2025), focus on selecting instances that are neither too hard nor too easy. Yet, these approaches heavily rely on rollouts, incurring substantial extra rollout costs. Conversely, methods such as GRESO (Zheng et al., 2025b) utilize historical training dynamics to estimate utility with negligible cost (Gao et al., 2025b; Sun et al., 2025b). While efficient, these metrics based on historical dynamics quickly become stale during training; as model parameters update, the shifting ‘state of

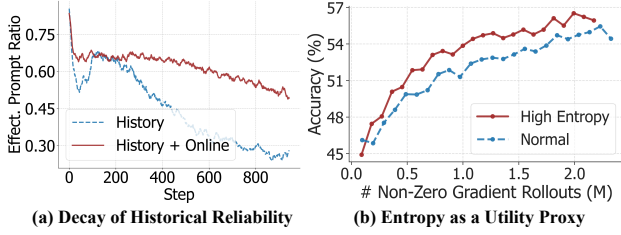


Figure 2. (a) History-based selection suffers from metadata staleness, leading to a decay in effective (non-zero gradient) prompts. Real-time verification (Online) prevents this, sustaining high sample validity. (b) Prioritizing high-entropy prompts among non-zero gradient prompts significantly improves accuracy compared to standard sampling, validating entropy as a key efficiency signal.

knowledge’ often leads previously informative prompts to become trivial, making historical indicators unreliable for real-time selection (Figure 2a).

To devise an efficient prompt selection framework for scaling rollouts in LLM RL, we begin by conducting an empirical analysis of training dynamics. Our findings reveal that sample utility is non-uniform and dynamic (Section 2). Specifically, among those prompts with effective gradients, high-entropy ones yield higher utility (Figure 2b). This aligns with the finding in Section 2: the strongest learning signals are concentrated at the “learning edge” defined by the intersection of medium difficulty and high response entropy (Figure 3). Furthermore, this utility is inherently changing; as the model updates, a phenomenon we term “metadata staleness” occurs. We observe that the group of prompts identified as informative by history-based metrics becomes ineffective for current training (Figure 3).

Based on these insights, we conclude that an ideal prompt selection framework for efficient LLM RL must satisfy three criterias: it must be **online** to track the model’s shifting learning edge, **precise** in identifying real-time utility of each prompts, and **computationally efficient** enough to ensure that the selection cost is minimal.

To meet these requirements, we propose **HIVE** (History-Informed and online-VERified prompt selection), a hierarchical framework designed for data-efficient LLM training (Figure 4). HIVE operates through a two-stage process: (1) leveraging historical reward trajectories and response entropies to prioritize informative prompts from the candidate pool; (2) utilizing prompt entropy as a high-fidelity and efficient proxy to resolve metadata staleness and select samples useful for the current model training. We evaluate HIVE across six math reasoning benchmarks and six models: Qwen2.5-Math-1.5B/7B (Yang et al., 2024), DeepSeek-R1-Distill-Qwen-1.5B (Guo et al., 2025), Qwen2.5-14B/32B (Team, 2024), and Llama-3.2-3B-Instruct (Grattafiori et al., 2024). HIVE significantly outperforms baselines like Dynamic Sampling and GRESO, achieving up to **3.8× speedup in rollout** and **2.2× faster**

**total training time** for models like Qwen2.5-Math-7B. Finally, we show that HIVE drastically lowers computational overhead, achieving **up to 9.2 million rollouts reduction** while consistently maintaining or even exceeding the reasoning accuracy of Dynamic Sampling and GRESO.

## 2. Background and Motivation

In this section, we dissect the learning dynamics of GRPO to identify the specific data characteristics that drive effective model updates. Specifically, our empirical analysis is structured around two fundamental questions: (1) Prompt Utility: Which specific groups of samples carry the most significant information for model optimization? (2) Temporal Dynamics: How does the utility of these samples shift and evolve during training? The insights gained from these observations directly inspire the design of HIVE.

**Zero Advantages in GRPO.** Group relative policy optimization (GRPO) (Shao et al., 2024) is a widely adopted policy gradient algorithm in reinforcement learning with verifiable rewards (RLVR) (Guo et al., 2025; Yang et al., 2025). Derived from proximal policy optimization (PPO) (Schulman et al., 2017), GRPO is tailored for fine-tuning language models. GRPO has exhibited superior performance in various tasks advances (Guo et al., 2025; Yang et al., 2025; Yu et al., 2025; Bai et al., 2024). The training objective of GRPO is as follows:

$$\mathcal{J}_{\text{GRPO}}(\theta) = \mathbb{E} \left[ q \sim P(Q), \{o_i\}_{i=1}^G \sim \pi_{\theta_{old}} \right] \left[ \frac{1}{G} \sum_{i=1}^G \frac{1}{|o_i|} \sum_{t=1}^{|o_i|} \left( \mathcal{L}_{i,t}^{\text{clip}}(\theta) - \beta D_{\text{KL}}(\pi_{\theta} \| \pi_{\text{ref}}) \right) \right], \quad (1)$$

where  $\mathcal{L}_{i,t}^{\text{clip}}(\theta)$  is the clipped surrogate objective defined as:

$$\mathcal{L}_{i,t}^{\text{clip}}(\theta) = \min \left( \rho_{i,t}(\theta) \hat{A}_{i,t}, \text{clip}(\rho_{i,t}, 1 \pm \epsilon) \hat{A}_{i,t} \right), \quad (2)$$

where  $\rho_{i,t}(\theta) = \frac{\pi_{\theta}(o_i|q)}{\pi_{\theta_{old}}(o_i|q)}$ , and  $\hat{A}_i$  is the advantage, computed from a group of rewards  $\{r_i\}_{i=1}^G$  as following:

$$\hat{A}_i = \frac{r_i - \text{mean}(\{R_i\}_{i=1}^G)}{\text{std}(\{R_i\}_{i=1}^G)}. \quad (3)$$

The advantage for each response is derived from the normalized reward within its respective group of sampled rollouts. Consequently, in cases where a prompt exhibits extreme difficulty or simplicity, the advantage vanishes as the rewards for all responses converge (i.e., all correct or all incorrect). This result yields a **zero gradient** for policy updates, thereby **providing no informative learning signal**.

**Utility: Difficulty and Entropy.** While prompts yielding zero gradients provide no informative signal for training (Guo et al., 2025; Shao et al., 2024), we take a further step to investigate which prompts among those with

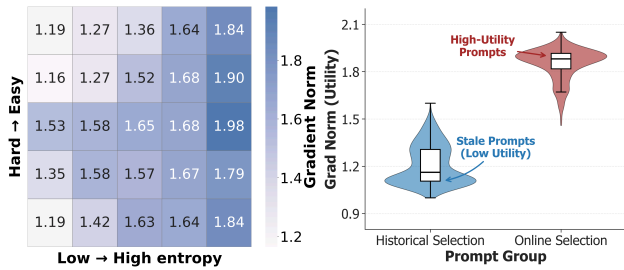


Figure 3. Left: Peak gradients (color intensity) appear in the intersection of high-entropy and intermediate difficulty regions, indicating the strongest learning signals. Right: Selection based on historical metrics yields stale prompts with lower utility.

non-zero gradients are most valuable for RL training. As Figure 2b suggests, non-zero gradient prompts with higher entropy can yield performance improvement with identical rollout cost. On the other hand, previous studies (Kim et al., 2025; Paul et al., 2021; Fayyaz et al., 2022; Singhal et al., 2024) reveal that length-normalized gradient norm can serve as an effective metric to measure the utility of prompts. Therefore, in this section, we focus on analyzing how *per-prompt difficulty* (empirical accuracy across rollouts) and *response entropy* correlate with the prompt utility, using the gradient as indicator.

As illustrated in the heatmap in Figure 3 (Left), two distinct trends emerge that define the topography of sample utility: (1) **Monotonicity in Entropy**: Within any fixed difficulty band, the gradient norm increases almost monotonically with response entropy. (2) **Inverted-U in Difficulty**: For a fixed entropy level, the gradient norm follows an “inverted-U” pattern relative to difficulty. Magnitude is minimized at the saturated prompts that are either trivial (always correct) or intractable (always incorrect), and peaks near the “learning edge”. **The global maximum of utility, evaluated by the normalized gradient norm, is concentrated in the high-entropy, medium-difficulty region** (e.g., the middle-right cells reaching  $\sim 1.98$ ). This suggests that a model’s learning trajectory is primarily driven by high-utility samples. Prioritizing prompts at the intersection of high entropy and medium accuracy can prevent rollout budgets from being wasted on samples that provide no discriminative signal.

**Staleness: Decay of Historical Reliability.** While historical metadata (e.g., response entropy, and reward trajectories) provides a useful prior for sample selection, its reliability is inherently transient (Cui et al., 2025; Tomihari, 2026; Li et al., 2026). As the model parameters update during training, the model’s “state of knowledge” shifts, causing the utility of specific prompts to decay, which we refer as data staleness.

To quantify this effect, we compare the utility of prompts selected based on historical metadata (reward trajectories and response entropies from last epoch) against those identified

by online metrics (variance of rewards in current rollouts and corresponding response entropies). As illustrated in Figure 3 (Right), we observe a sharp divergence in the resulting gradient norms. The prompts chosen via *Historical Selection* exhibit significantly lower gradient norms (clustering around 1.2), indicating they have degraded into “stale prompts” that provide diminished learning signals. In contrast, *Online Selection* consistently isolates “High-Utility Prompts” with elevated gradient norms (median  $\approx 1.9$ ). This empirical gap underscores that **metrics derived from the historical training trajectory rapidly lose their validity as proxies for real-time selection**, as they fail to track the model’s shifting learning edge. Thus, metrics derived from the historical training trajectory may no longer serve as valid proxies for prompt selection in the current iteration.

### 3. Methodology

In this section, we present HIVE (**H**istory-**I**nformed and **V**erified prompt selection), a hierarchical framework designed to improve RL training efficiency by identifying high-utility prompts. As motivated by the observations in Section 2, HIVE selects prompts through a two-stage process. It first leverages historical training dynamics (e.g., reward trajectories and response entropies) for cost-free coarse selection, followed by an online verification stage that utilizes real-time prompt entropy to ensure the current relevance of selected samples before rollout phase. The overall framework is shown in Figure 4 and the detailed algorithm can be found in the Appendix E.

#### 3.1. Stage 1: History-Informed Selection

Stage 1 involves a zero-cost, history-informed mechanism to select high-utility prompts. Based on the observation from Section 2, we define high-utility prompts as those with intermediate difficulty and high entropy. To avoid redundant rollout costs, we quantify the prompt difficulty by reward-trajectories and predictive diversity by response entropies from previous iterations. To prevent the model from prematurely discarding prompts that may become solvable as training progresses, we adopt a probabilistic selection strategy based on reward-trajectories (reward-based score) and response entropies (entropy-based score).

**Reward-based Score.** Given a historical training dynamics trace  $T_i$  for each prompt  $x_i \in \mathcal{D}$ :

$$T_i = \{R_{i,1}, \dots, R_{i,n}\}, \quad (4)$$

where  $R_{i,j} = \{r_{i,j}^{(k)}\}_{k=1}^G$  represents the set of response rewards obtained from  $G$  rollouts in  $j$ -th epoch. As analyzed in Section 2, prompts that consistently yield zero reward variance provide vanishing gradients and offer no informative signal for model updates. We quantify this lack of informativeness by tracking the consecutive zero-variance

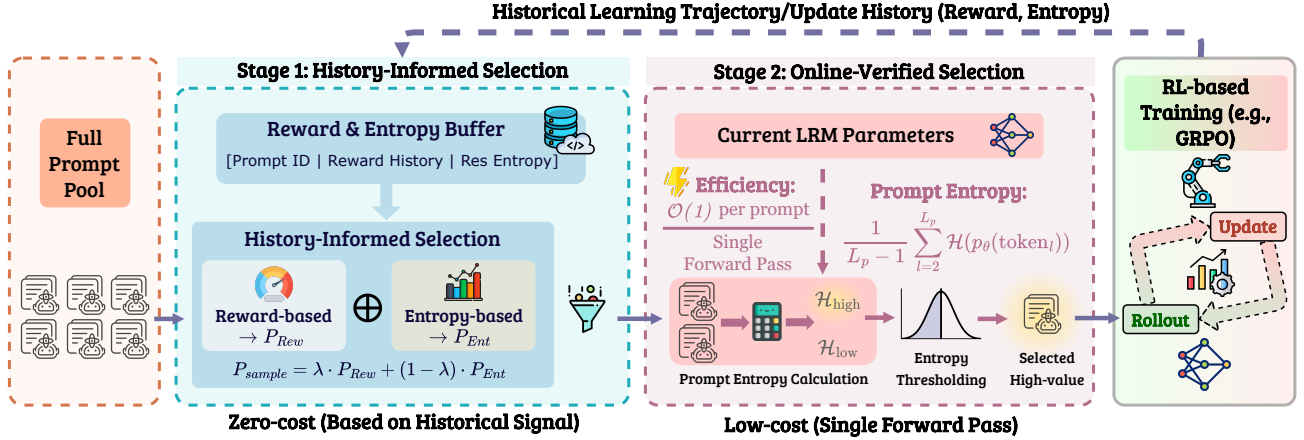


Figure 4. Overview of the Proposed Framework. (1) Stage 1: History-Informed Selection utilizes reward histories and response entropies from historical rollouts to define the probability of selecting high-utility prompts at “learning edge”. (2) Stage 2: Online-Verified Selection calculates prompt entropies based on the current LRM parameters and select those in target range for training.

count  $z_i$ , which represents the number of most recent consecutive iterations where  $x_i$  yielded identical rewards:

$$z_i = \max\{k \in [0, n] \mid \prod_{j=n-k+1}^n \mathbb{I}_{i,j} = 1\}, \quad (5)$$

where  $\mathbb{I}_{i,j}$  is an indicator function that equals 1 if all rewards in  $R_{i,j}$  are identical, and 0 otherwise. The prompt selection probability based on reward trajectories is defined as:

$$P_{Rew}(x_i) = p_e^{z_i}, \quad (6)$$

where  $p_e \in (0, 1)$  is the base exploration probability. This mechanism ensures that prompts frequently identified as zero-variance are pruned with increasing probability, while still allowing for occasional re-sampling to account for shifts in the model’s “learning edge”.

Manually determined  $p_e$  can always be trivial when applied across models, datasets, and training stages. HIVE employs an adaptive mechanism to automatically adjust the base exploration probability at each training iteration. Specifically, HIVE monitors the observed zero-variance ratio against a target  $\alpha$ . If the actual ratio of uninformative rollouts exceeds the target,  $p_e$  decreases by step size  $\Delta p$  to lower sampling intensity; otherwise, it increases. Furthermore, HIVE maintains decoupled probabilities,  $p_{e,easy}$  and  $p_{e,hard}$ , to independently track easy and hard prompts.

**Entropy-based Score.** The entropy-based score further refines selection by prioritizing samples with high predictive uncertainty. We define the historical response entropy for a prompt  $x_i$ , denoted as  $H_i$ , as the average of the mean token-level entropies across  $G$  independent rollouts generated in the most recent epoch. Specifically, for each rollout  $r \in \{1, \dots, G\}$ , the model generates a response sequence of length  $L_r$ . Let  $p_{\theta,l}^{(r)} = p_{\theta}(\cdot | x_{<l}^{(r)})$  be the token probability

distribution given context  $x_{<l}^{(r)}$ . Mean entropy of the  $r$ -th rollout  $U^{(r)}(x_i)$  and historical entropy  $H_i$  is calculated as:

$$H_i = \frac{1}{G} \sum_{r=1}^G U^{(r)}(x_i), \quad U^{(r)}(x_i) = \frac{1}{L_r} \sum_{l=1}^{L_r} \mathcal{H}(p_{\theta,l}^{(r)}), \quad (7)$$

where  $L_r$  is the length of  $r$ -th rollout and  $\mathcal{H}(p_{\theta,l}^{(r)})$  is the token level entropy at position  $l$ :

$$\mathcal{H}(p_{\theta}(\cdot | x_{<l}^{(r)})) = - \sum_{v \in \mathcal{V}} p_{\theta}(v | x_{<l}^{(r)}) \log p_{\theta}(v | x_{<l}^{(r)}). \quad (8)$$

To map the historical entropy  $H_i$  into a selection probability  $P_{Ent}(x_i)$ , we employ a scoring mechanism that favors high-entropy candidates:

$$P_{Ent}(x_i) = \frac{H_i - H_{min}}{H_{max} - H_{min}}, \quad (9)$$

where  $H_{max}$  and  $H_{min}$  are the maximum and minimum average response entropies in the current epoch, respectively.

**History-Informed Selection.** To identify the learning edge, HIVE integrates both reward and entropy signals. While the reward-based score  $P_{Rew}$  reflects the learning outcome (i.e., whether the model has already mastered or is currently stuck on a prompt), the entropy-based score  $P_{Ent}$  captures the internal confidence of the model’s policy. By combining them, the final probability of selecting prompt  $x_i$  is calculated as:

$$P_{select} = \lambda \cdot P_{Rew}(x_i) + (1 - \lambda) \cdot P_{Ent}(x_i), \quad (10)$$

where  $\lambda$  is a balancing coefficient.

### 3.2. Stage 2: Online-Verified Selection

As motivated by the staleness analysis in Section 2, historical metrics may fail to reflect the model’s current “state of

knowledge” and select effective prompts for training. Thus, we choose to devise online metrics for prompt selection. However, calculating the full response entropies and rollouts for every candidate is computationally prohibitive. To bridge this gap, stage 2 introduces an online verification phase. Unlike the soft selection in stage 1, this stage acts as a deterministic gatekeeper: it re-verifies the utility of candidate prompts using the current policy before any expensive rollouts occur. To bridge this gap without incurring significant overhead, stage 2 introduces a lightweight online verification phase. Instead of expensive response generation, we pivot to using *online prompt entropy* as a high-fidelity, efficient proxy to select candidates before the rollout phase.

**Prompt Entropy as a Proxy.** Formally, we define the prompt entropy  $V(x)$  as the average of token-level entropy across the prompt sequence:

$$V(x) := \frac{1}{L_p - 1} \sum_{l=2}^{L_p} \mathcal{H}(p_\theta(\cdot|x_{<l})), \quad (11)$$

where  $L_p$  is the prompt length and  $\mathcal{H}(p_\theta(\cdot|x_{<l}))$  is the token entropy at position  $l$ .

To rigorously justify the use of prompt-side entropy  $V(x)$  as a proxy for response-side utility  $U(x)$ , we establish a theoretical guarantee of **Rank Consistency**. Under the assumptions of *Representation Approximation* and *Entropy Propagation* (see Appendix A.2 for detailed formulations), we provide the following main result:

**Theorem 3.1** (Informal). *For any pair of prompts  $(x, x')$ , if the difference in their prompt-side entropy  $\Delta V$  exceeds a specific noise-related threshold, then their ranking in  $V(x)$  is consistent with their ranking in the true expected response entropy  $U(x)$  with high probability:*

$$\text{sign}(V(x) - V(x')) = \text{sign}(\hat{U}(x) - \hat{U}(x')). \quad (12)$$

This theorem (formally presented as Theorem A.4 in the Appendix A) ensures that  $V(x)$  is a theoretically sound estimator for tracking the model’s current learning edge. The theoretical proof is examined in Appendix A.

**Entropy-based Selection.** Following the online calculation, HIVE implements a deterministic gate to finalize selection. To maintain adaptability as the LLM updates, we employ a dynamic median-based threshold. Let  $\mathcal{D}_{S1}$  be the candidate set passing Stage 1. We define the verification threshold  $\gamma$  as the median prompt entropy of the current pool:

$$\gamma := \text{median}(V(x) \mid x \in \mathcal{D}_{S1}). \quad (13)$$

A prompt  $x_i$  is promoted to the rollout phase if it satisfies:

$$x_i \in \mathcal{D}_{S1} \quad \text{and} \quad V(x_i) \geq \gamma. \quad (14)$$

This “soft-to-hard” selection ensures a constant relative throughput, forcing the model to prioritize the top 50% most informative samples. By validating historical utility with online prompt entropy, HIVE resolves metadata staleness and maximizes gradient utility per rollout.

**Computational Efficiency.** Stage 2 achieves extreme efficiency by replacing multi-sample rollouts with a *single forward pass* over the prompt tokens. For a prompt of length  $L_p$ , group size  $G$  and response length  $L_r$ , calculating  $V(x)$  only needs one forward pass, whereas a full group rollout requires  $G \cdot L_r$  forward passes. Specifically, this reduces the computational complexity from  $O(G \cdot L_r)$  to  $O(1)$ . By selecting prompts with high  $V(x)$ , HIVE effectively resolves the metadata staleness issue while bypassing the prohibitive costs of full rollouts. The time cost of Stage 2 is empirically verified as negligible, shown in Figure 6d in Section 4.3.

## 4. Experiments

In this section, we evaluate HIVE on multiple benchmarks across six different models:

- In Section 4.2, we show that HIVE achieves significant rollout reduction with no performance degradation.
- In Section 4.3, we conduct a detailed analysis of how HIVE reduces training costs by identifying effective prompts for rollout and other training dynamics
- In Section 4.4, we conduct investigation on the effects of HIVE’s different stages.

### 4.1. Experimental Settings

**Models & Datasets.** We run our experiments on Qwen2.5-Math-1.5B/7B (Yang et al., 2024), DeepSeek-R1-Distill-Qwen-1.5B (Guo et al., 2025), Qwen2.5-14B/32B (Team, 2024), and Llama-3.2-3B-Instruct (Grattafiori et al., 2024). We use a context length of 4K for Qwen2.5-Math-1.5B/7B, and 8K for DeepSeek-R1-Distill-Qwen-1.5B and Llama-3.2-3B-Instruct. For Qwen2.5-14B/32B models, we set the context length to 16k. For training datasets, we adopt two datasets following Zheng et al. (2025b): 1) DAPO+MATH (DM): It is the combination of DAPO dataset (Yu et al., 2025) and MATH dataset (Hendrycks et al., 2021). 2) OPEN-R1 30k subset (OR1): 30,000-example subset of the OPEN-R1 math dataset (Hugging Face, 2025).

**Training & Evaluation.** Our method is implemented based on verl (Sheng et al., 2025b) and vLLM (Kwon et al., 2023). We use  $8 \times A100-80G$  GPUs for Qwen2.5-Math-1.5B/7B, DeepSeek-R1-Distill-Qwen-1.5B and Llama-3.2-3B-Instruct in the main experiments. For benchmark datasets, we use six widely used complex mathematical reasoning benchmarks to evaluate the performance of trained models: Math500 (Hendrycks et al., 2021), AIME24 (Art

Table 1. Comprehensive evaluation of HIVE on math reasoning benchmarks and efficiency analysis. We train four models on DAPO + MATH. (a) Compared to Dynamic Sampling (DS) and GRESO, HIVE achieves similar accuracy while significantly reducing the number of rollouts. (b) HIVE significantly lowers rollout cost, achieving up to 3.8× speedup in rollout, 2.2× speedup in total training cost over Dynamic Sampling, and consistently outperforming GRESO.

(a) Performance (%) comparison across six math reasoning benchmarks.									(b) Training time (hours) comparison.				
Method	Math500	AIME24	AMC	Gaokao	Miner.	Olymp.	Avg.	#Rollout	Method	Train	Other	Rollout	Total
<i>Qwen2.5-Math-1.5B</i>									<i>Qwen2.5-Math-1.5B</i>				
DS	77.3	16.7	61.7	64.2	31.8	38.7	48.4	7.6M (1.0×)	DS	10.9	6.0	77.3	94.2
GRESO	77.3	15.0	59.3	66.2	32.6	38.5	48.1	3.3M (2.3×)	GRESO	11.3	6.4	46.0	63.7
Our	77.9	16.7	60.2	66.1	31.5	40.3	48.8	<b>3.1M (2.5×)</b>	Our	11.2	6.2	<b>42.1</b>	<b>59.5</b>
<i>DeepSeek-R1-Distill-Qwen-1.5B</i>									<i>DeepSeek-R1-Distill-Qwen-1.5B</i>				
DS	87.9	36.7	71.7	78.7	35.3	54.9	60.9	2.4M (1.0×)	DS	9.6	6.1	68.7	84.4
GRESO	85.5	37.5	70.7	76.2	34.3	52.1	59.4	1.6M (1.5×)	GRESO	10.4	6.6	45.9	62.9
Our	87.2	37.5	70.1	77.2	35.1	53.2	60.1	<b>1.5M (1.6×)</b>	Our	10.1	6.7	<b>42.7</b>	<b>59.5</b>
<i>Llama3.2-3b-Instruct</i>									<i>Llama3.2-3b-Instruct</i>				
DS	52.4	16.7	46.0	49.2	20.0	20.2	34.1	11.4M (1.0×)	DS	20.6	10.2	218.3	249.1
GRESO	51.8	16.7	46.3	49.4	19.7	19.6	33.9	5.9M (1.9×)	GRESO	21.8	10.5	116.5	148.8
Our	53.8	17.5	45.5	49.1	20.5	20.0	34.4	<b>4.8M (2.4×)</b>	Our	22.2	10.6	<b>90.4</b>	<b>123.2</b>
<i>Qwen2.5-Math-7B</i>									<i>Qwen2.5-Math-7B</i>				
DS	82.9	34.2	79.2	71.7	35.4	43.6	57.8	13.1M (1.0×)	DS	32.1	12.6	153.7	198.4
GRESO	93.2	30.0	78.9	70.2	35.2	44.1	58.6	6.3M (2.1×)	GRESO	32.8	13.2	66.3	112.3
Our	93.0	36.7	79.2	70.8	34.8	43.8	59.7	<b>3.9M (3.4×)</b>	Our	32.7	12.9	<b>40.2</b>	<b>85.8</b>

of Problem Solving, 2024a), AMC (Art of Problem Solving, 2024b), Minerva Math (Lewkowycz et al., 2022), Gaokao (Zhang et al., 2023), and Olympiad Bench (He et al., 2024). Following (Zheng et al., 2025b), we report the performance of the checkpoint that obtains the best average performance on six benchmarks. We also include more detailed settings in Appendix B.

#### 4.2. Efficiency Comparison (Table 1 & 2, Figure 5)

**Comparable performance with up to 3.4× fewer rollouts (Table 1a & 2).** We evaluate the performance of HIVE against two distinct baselines: Dynamic Sampling (DS) (Yu et al., 2025), which filters out zero-variance examples and resamples to fill the batch with effective data, and GRESO (Zheng et al., 2025b), a prevalent history-based selection method. Table 1a presents the comparative results across four LLMs, trained on DAPO + MATH dataset, and they are evaluated on six mathematical reasoning benchmarks. We report both the best average performance across six benchmarks and the accumulated number of rollouts over 1000 training steps. HIVE consistently reduces the number of rollouts and matches or exceeds the accuracy of DS and GRESO across all model architectures. For instance, on *Qwen2.5-Math-7B*, HIVE reduces rollouts by 70% compared to DS (13.1M → 3.9M), achieving a 3.4× speedup that surpasses GRESO (2.1×). At the same time, it achieves the highest average accuracy of 59.7%, outperforming GRESO (58.6%) and DS (57.8%). This confirms the effectiveness of HIVE in selecting prompts for training efficiency. Such advancements are also observed on other

models and training on dataset OpenR1 (Table 2).

**Up to 3.8× wall-clock time speed-up in rollout and 2.2× speed-up in training (Table 1b).** To better understand the efficiency of HIVE, we report the detailed end-to-end training time (1000 steps) breakdown for different stages. All the models are trained on 8×A100. Table 1b shows that HIVE significantly reduces the computational overhead of training across all settings (1.5B to 7B parameters). While rollout is the primary computational cost in the RL-based training, HIVE achieves a rollout speedup of up to 3.8× (153.7h→40.2h) and a total training speedup of up to 2.3× (198.4h→85.8h). For instance, HIVE reduces total training time of *Qwen2.5-Math-7B* from 198.4 hours (DS) and 112.3 hours (GRESO) to 85.8 hours, and reduces rollout time from 153.7 hours (DS) and 66.3 hours (GRESO) to 40.2 hours.

**Scaling 14B and 32B Models (Figure 5).** We extend our evaluation to the *Qwen-2.5-14B* and *32B* models to verify HIVE’s effectiveness at larger scales. The reported results in Figure 5 show the average performance across the six benchmarks. HIVE exhibits a convergence trajectory similar to both DS and GRESO, ensuring no compromise in final performance. However, HIVE requires fewer rollouts. For example, for the training of *Qwen-2.5-14B* over 800 steps, HIVE requires only 1.56M rollouts, significantly less than GRESO (1.74M) and Dynamic Sampling (3.45M).

#### 4.3. Further Efficiency Analysis (Figure 6 & 7)

**Computational cost of online-verified selection (Stage 2) is negligible (Figure 6a).** The figure presents a break-

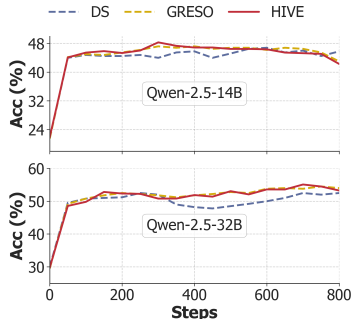
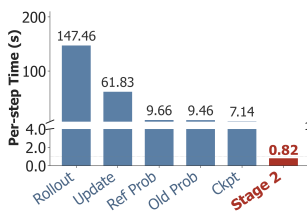


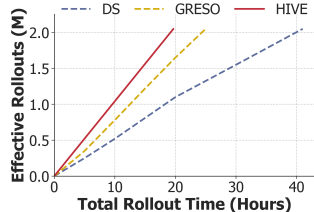
Figure 5. Accuracy comparison on Qwen2.5-14B and Qwen2.5-32B.

Table 2. Performance (%) comparison of Qwen2.5-Math-1.5B and Qwen2.5-Math-7B trained on OpenR1.

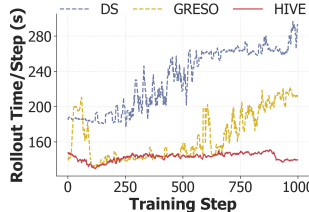
Method	Math500	AIME24	AMC	Gaokao	Miner.	Olymp.	Avg.	#Rollout
<i>Qwen2.5-Math-1.5B</i>								
DS	77.1	16.7	50.3	65.5	30.9	39.7	46.7	3.8M (1.0×)
GRESO	76.1	20.0	50.6	65.1	30.0	39.2	46.8	1.6M (2.4×)
Our	76.9	18.3	48.7	65.4	30.1	40.3	46.6	<b>1.5M (2.5×)</b>
<i>Qwen2.5-Math-7B</i>								
DS	82.8	34.2	63.5	67.3	35.7	46.3	55.0	11.4M (1.0×)
GRESO	82.3	35.0	64.4	66.8	36.5	45.7	55.1	3.4M (3.4×)
Our	82.6	36.7	63.9	66.7	36.2	45.9	55.3	<b>2.5M (4.7×)</b>



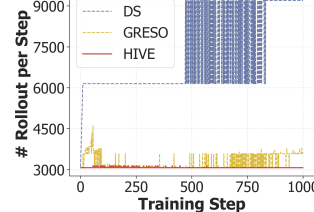
(a) Training Time Breakdown



(b) Efficiency Comparison



(c) Generation Time



(d) Rollouts per Step

Figure 6. Efficiency analysis of Qwen-Math-1.5B trained on the DAPO + MATH dataset. (a) Blue bars indicate shared components with DS and GRESO. Red bars show HIVE-specific additional time consuming. (b) Comparison of the accumulation of valid rollouts over rollout hours; HIVE achieves the fastest accumulation rate. (c) HIVE maintains low latency throughout training, whereas GRESO and DS incur significantly higher time costs. (d) HIVE consistently rollouts for fewer prompts per step than DS and GRESO.

down of the wall-clock time per training step (averaged over the first 20 steps). The computational cost is heavily dominated by standard components shared with baselines (DS and GRESO), specifically the Rollout (147.46s) phase. In contrast, the calculation of online prompt entropy in the stage 2 (online-verified selection) of HIVE, introduces a marginal latency of only 0.82s. This demonstrates that the online-verified selection enhances performance with negligible computational cost (<0.4% of the total iteration time).

**HIVE yields better rollout efficiency and effective rollout ratios (Figure 6b, 6c, 6d).** We analyze the temporal dynamics of rollout generation in Figures 6b to 6d to validate the computational advantages of HIVE. As shown in Figure 6b, HIVE (red line) exhibits the steepest accumulation of effective rollouts per hour. This also confirms that the overhead of Stage 2 online verification is negligible compared to the significant throughput gains achieved by avoiding redundant rollouts. Figure 6c reveals a critical divergence: HIVE maintains consistently low latency (145s/step), whereas GRESO suffers from increasing costs later in training (>200s/step). This degradation highlights the impact of metadata staleness; history-based methods fail to filter increasingly complex yet uninformative prompts as the model evolves. Figure 6d demonstrates that HIVE have the strictest selection volume, therefore yielding the least waste of rollout. By avoiding the increasing seen in

DS and GRESO, HIVE ensures computational resources are focused on the effective prompts near “learning edge”.

**Dynamics of uninformative prompts (Figure 7).** We analyze the zero-variance ratio to measure the proportion of selected prompts that yield zero gradients (uninformative signals). The results are presented in Figure 7. As the model improves, Dynamic Sampling (DS) wastes nearly 50% of rollouts on easy problems. GRESO fails to filter these effectively due to metadata staleness, while its historical records lag behind the newly updated model. In contrast, HIVE consistently maintains a low ratio. For “hard” samples, HIVE converges at a lower zero-variance ratio than baselines. By aggressively filtering both easy and hard extremes, HIVE ensures that the computational budget is concentrated exclusively on the most informative prompts.

4.4. Component Study (Figure 8)

**Threshold dynamics (Figure 8a).** The reported result tracks the adaptive entropy threshold  $\gamma$ , which monotonically decreases from 1.3 to 0.35. This decline mirrors the model’s increasing confidence. By dynamically lowering  $\gamma$ , HIVE continuously tracks the shifting “learning edge”, ensuring selection criteria remains strict as the model matures to prevent the over-sampling of easy instances.

**Ablation study on two stages (Figure 8b).** We quantify the

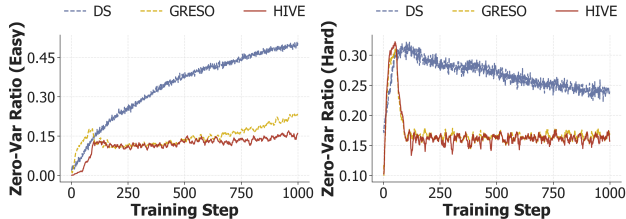


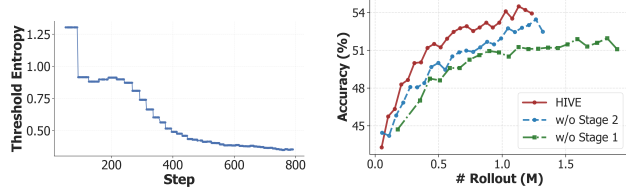
Figure 7. Evolution of zero-variance ratios (lower indicates more effective prompts selected). HIVE (red) consistently minimizes the selection of uninformative prompts, both easy and hard.

impact of each stage in Figure 8b. *w/o Stage 2 (Blue)*: Removing online verification degrades efficiency, confirming that historical metrics alone suffer from metadata staleness and waste computation on outdated prompts. *w/o Stage 1 (Green)*: Removing historical selection yields the lowest efficiency, proving that a zero-cost “coarse” filter is necessary to prune obvious noise before verification. *HIVE (Red)*: The full framework dominates the pareto frontier, demonstrating that the synergy between historical priors and online verification is essential for maximizing rollout efficiency.

## 5. Related Works

**RL for LLM Reasoning.** Reinforcement learning (RL) is central to post-training LLMs (Christiano et al., 2017; Bai et al., 2022) and recent work prioritizes reinforcement learning with verifiable rewards (RLVR) (Ouyang et al., 2022; Rafailov et al., 2023; Guo et al., 2025; Hu, 2025; Liu et al., 2025; Jaech et al., 2024; Zhang et al., 2025c). Recent methods are in two main categories: (1) Value-enhanced PPO, where algorithms like VC-PPO (Yuan et al., 2025) and VAPO (Yue et al., 2025) improve reasoning by strengthening value-function learning; and (2) Group-based Policy Optimization, where methods like RLOO (Ahmadian et al., 2024) and GRPO (Shao et al., 2024) employ multi-sample baselines to bypass explicit value learning for efficiency. To further stabilize training, recent works have introduced experience replay (Liang et al., 2025; Li et al., 2025a; Zhang et al., 2025b) or modified optimization objectives to mitigate bias (Dr. GRPO (Liu et al., 2025)) and enhance sequence-level regulation (GSPO (Zheng et al., 2025a)). DAPO (Yu et al., 2025) attempts to filter zero-gradient instances based on computationally cost rollouts.

**Data Efficient LLM Training.** Data curation is critical for efficient reinforced fine-tuning. Following the “less is more” principle (Zhou et al., 2023; Ye et al., 2025b), small, high-quality datasets often outperform large, noisy corpora (Wang et al., 2025b; Fatemi et al., 2025; Li et al., 2025b; Shi et al., 2025; Tang et al., 2025). Online selection methods have emerged to dynamically select data, falling into three types: (1) Rollout-based Selection: Discarding uninformative prompts via real-time sampling (Yu et al.,



(a) Threshold Entropy (Stage 2) (b) Ablation Study

Figure 8. (a) shows the response gamma entropy decreasing over steps. (b) compares the accuracy across different ablation settings.

2025; Meng et al., 2025; Foster et al., 2025; Xu et al., 2025; Lin et al., 2025; Sun et al., 2025a; Bae et al., 2025). This incurs high computational overhead. (2) Estimator-based Selection: Utilizing historical logs (Zheng et al., 2025b) or Bayesian estimators (Chen et al., 2025b; Zeng et al., 2025; Shen et al., 2025) to predict utility, suffering from memory overhead or estimation errors. (3) Auxiliary-Model Selection: Employing external scorers (DOTS (Sun et al., 2025c)) or on-policy value models (PCL (Gao et al., 2025c)) to infer difficulty, adding compute costs. Alternatively, stage-wise curation (Zhang et al., 2025a;c) periodically refreshes data but fail to track real-time learning dynamics. In contrast, our method devises a low-cost, real-time selection stage to precisely identify and retain prompts at the model’s learning edge. Detailed related work is in Appendix C.

## 6. Conclusion

Reinforcement learning with verifiable rewards is becoming vital for advancing the reasoning abilities of large language models. Training algorithms should prioritize high-utility samples rather than indiscriminately scaling rollouts. The key insight of HIVE to select useful prompts is to precisely target the moving “learning edge” and use online prompt entropy to verify the utility. Through extensive evaluations on math reasoning benchmarks, we demonstrate that HIVE is highly effective, significantly reducing computational costs of rollouts without performance drop.

## 7. Limitations

First, our current evaluation is restricted to text-based large reasoning models (LRMs). We have not yet explored how the principle of prompt entropy as a utility proxy translates to multi-modal contexts, such as vision-language models (VLMs). Extending HIVE to multi-modal scenarios represents a promising direction for future work. Second, HIVE introduces specific hyperparameters, such as the balancing coefficient  $\lambda$  and the adaptive step size  $\Delta p$ . Although our adaptive mechanism effectively mitigates the need for manual tuning, we have not performed an exhaustive grid search to guarantee global optimality for these parameters across all possible training scales.

## Impact Statements

This paper presents work whose goal is to advance the field of machine learning. The introduced framework (HIVE) has the potential to improve the data and computational efficiency of reinforcement learning for large language models in a wide range. HIVE directly contributes to Green AI by lowering the energy consumption and carbon footprint associated with training large reasoning models. Additionally, by reducing computational barriers, this work promotes the democratization of research, enabling smaller academic groups with limited resources to participate in advanced model fine-tuning. We do not foresee specific negative societal consequences beyond the general risks associated with advancing data-efficient training for LLM reasoning.

## References

- Ahmadian, A., Cremer, C., Gallé, M., Fadaee, M., Kreutzer, J., Pietquin, O., Üstün, A., and Hooker, S. Back to basics: Revisiting reinforce style optimization for learning from human feedback in llms. *arXiv preprint arXiv:2402.14740*, 2024.
- Art of Problem Solving. AIME problems and solutions. [https://artofproblemsolving.com/wiki/index.php/AIME\\_Problems\\_and\\_Solutions](https://artofproblemsolving.com/wiki/index.php/AIME_Problems_and_Solutions), 2024a.
- Art of Problem Solving. AMC problems and solutions. [https://artofproblemsolving.com/wiki/index.php?title=AMC\\_Problems\\_and\\_Solutions](https://artofproblemsolving.com/wiki/index.php?title=AMC_Problems_and_Solutions), 2024b.
- Bae, S., Hong, J., Lee, M. Y., Kim, H., Nam, J., and Kwak, D. Online difficulty filtering for reasoning oriented reinforcement learning. *arXiv preprint arXiv:2504.03380*, 2025.
- Bai, J., Bai, S., Yang, S., Wang, S., Tan, S., Wang, P., Lin, J., Zhou, C., and Zhou, J. Qwen-VL: A versatile vision-language model for understanding, localization, text reading, and beyond. In *Proceedings of the Twelfth International Conference on Learning Representations (ICLR)*, 2024.
- Bai, Y., Jones, A., Ndousse, K., Askell, A., Chen, A., Das-Sarma, N., Drain, D., Fort, S., Ganguli, D., Henighan, T., et al. Training a helpful and harmless assistant with reinforcement learning from human feedback. *arXiv preprint arXiv:2204.05862*, 2022.
- Chen, W., Koenig, S., and Dilkina, B. Lspo: Length-aware dynamic sampling for policy optimization in llm reasoning. *arXiv preprint arXiv:2510.01459*, 2025a.
- Chen, X., Lu, J., Kim, M., Zhang, D., Tang, J., Piché, A., Gontier, N., Bengio, Y., and Kamaloo, E. Self-evolving curriculum for llm reasoning. *arXiv preprint arXiv:2505.14970*, 2025b.
- Christiano, P. F., Leike, J., Brown, T., Martic, M., Legg, S., and Amodei, D. Deep reinforcement learning from human preferences. In *Proceedings of Advances in Neural Information Processing Systems (NeurIPS)*, 2017.
- Chu, X., Huang, H., Zhang, X., Wei, F., and Wang, Y. Gpg: A simple and strong reinforcement learning baseline for model reasoning. *arXiv preprint arXiv:2504.02546*, 2025.
- Cui, G., Zhang, Y., Ouyang, W., Cheng, Y., Zhou, B., Ding, N., et al. The entropy mechanism of reinforcement learning for reasoning language models. *arXiv preprint arXiv:2505.22617*, 2025.
- Fatemi, M., Rafiee, B., Tang, M., and Talamadupula, K. Concise reasoning via reinforcement learning. *arXiv preprint arXiv:2504.05185*, 2025.
- Fayyaz, M., Aghazadeh, E., Modarressi, A., Pilehvar, M. T., Yaghoobzadeh, Y., and Kahou, S. E. Bert on a data diet: Finding important examples by gradient-based pruning. In *Proceedings of Advances in Neural Information Processing Systems (NeurIPS)*, 2022.
- Foster, T., Sims, A., Forkel, J., Fellows, M., and Foerster, J. Learning to reason at the frontier of learnability. *arXiv preprint arXiv:2502.12272*, 2025.
- Gao, S., Gong, T., Lin, Z., Xu, R., Zhou, H., and Li, J. Flue: Streamlined uncertainty estimation for large language models. In *Proceedings of the Thirty-Ninth AAAI Conference on Artificial Intelligence*, 2025a.
- Gao, Z., Kim, J., Sun, W., Joachims, T., Wang, S., Pang, R. Y., and Tan, L. Prompt curriculum learning for efficient llm post-training. *arXiv preprint arXiv:2510.01135*, 2025b.
- Gao, Z., Kim, J., Sun, W., Joachims, T., Wang, S., Pang, R. Y., and Tan, L. Prompt curriculum learning for efficient llm post-training. *arXiv preprint arXiv:2510.01135*, 2025c.
- Grattafiori, A. et al. The llama 3 herd of models. *arXiv preprint arXiv:2407.21783*, 2024.
- Guo, D., Yang, D., Zhang, H., Song, J., Zhang, R., Xu, R., Zhu, Q., Ma, S., Wang, P., Bi, X., et al. Deepseek-r1: Incentivizing reasoning capability in llms via reinforcement learning. *arXiv preprint arXiv:2501.12948*, 2025.
- He, C., Luo, R., Bai, Y., Hu, S., Thai, Z., Shen, J., Hu, J., Han, X., Huang, Y., Zhang, Y., Liu, J., Qi, L., Liu, Z., and

- Sun, M. OlympiadBench: A challenging benchmark for promoting AGI with olympiad-level bilingual multimodal scientific problems. In *Proceedings of the 62nd Annual Meeting of the Association for Computational Linguistics (ACL)*, 2024.
- Hendrycks, D., Burns, C., Kadavath, S., Arora, A., Basart, S., Tang, E., Song, D., and Steinhardt, J. Measuring mathematical problem solving with the math dataset. *arXiv preprint arXiv:2103.03874*, 2021.
- Hoefding, W. Probability inequalities for sums of bounded random variables. *Journal of the American Statistical Association*, 1963.
- Hu, J. Reinforce++: A simple and efficient approach for aligning large language models. *arXiv preprint arXiv:2501.03262*, 2025.
- Huang, W., Zhang, Q., Fang, Y., Liang, J., Rong, X., Yao, H., Wan, G., Liang, K., He, W., Li, M., et al. Mapo: Mixed advantage policy optimization. *arXiv preprint arXiv:2509.18849*, 2025.
- Hugging Face. Open r1: A fully open reproduction of deepseek-r1, January 2025. URL <https://github.com/huggingface/open-r1>.
- Jaech, A., Kalai, A., Lerer, A., Richardson, A., El-Kishky, A., Low, A., Helyar, A., Madry, A., Beutel, A., Carney, A., et al. Openai o1 system card. *arXiv preprint arXiv:2412.16720*, 2024.
- Kim, H., Oh, S., and Lee, S. Mitigating length bias in rlhf through a causal lens. *arXiv preprint arXiv:2511.12573*, 2025.
- Kwon, W., Li, Z., Zhuang, S., Sheng, Y., Zheng, L., Yu, C. H., Gonzalez, J., Zhang, H., and Stoica, I. Efficient memory management for large language model serving with pagedattention. In *Proceedings of the 29th Symposium on Operating Systems Principles (SOSP)*, 2023.
- Lewkowycz, A., Andreassen, A., Dohan, D., Dyer, E., Michalewski, H., et al. Solving quantitative reasoning problems with language models. In *Proceedings of Advances in Neural Information Processing Systems (NeurIPS)*, 2022.
- Li, S., Zhou, Z., Lam, W., Yang, C., and Lu, C. Repo: Replay-enhanced policy optimization. *arXiv preprint arXiv:2506.09340*, 2025a.
- Li, X., Zou, H., and Liu, P. Limr: Less is more for rl scaling. *arXiv preprint arXiv:2502.11886*, 2025b.
- Li, Z., Jiang, L., Hu, Y., Zeng, X., Li, Y., Zhang, X., Chen, G., Pan, Z., Li, X., and Liu, Y. No more stale feedback: Co-evolving critics for open-world agent learning. *arXiv preprint arXiv:2601.06794*, 2026.
- Liang, J., Tang, H., Ma, Y., Liu, J., Zheng, Y., Hu, S., Bai, L., and Hao, J. Squeeze the soaked sponge: Efficient off-policy reinforcement finetuning for large language model. *arXiv preprint arXiv:2507.06892*, 2025.
- Lin, Z., Lin, M., Xie, Y., and Ji, R. Cppo: Accelerating the training of group relative policy optimization-based reasoning models. *arXiv preprint arXiv:2503.22342*, 2025.
- Liu, Z., Chen, C., Li, W., Qi, P., Pang, T., Du, C., Lee, W. S., and Lin, M. Understanding r1-zero-like training: A critical perspective, 2025. *arXiv preprint arXiv:2503.20783*, 2025.
- Loshchilov, I. and Hutter, F. Decoupled weight decay regularization. In *Proceedings of the Seventh International Conference on Learning Representations (ICLR)*, 2019.
- Lu, N., Liu, S., Wu, J., Chen, W., Zhang, Z., Ong, Y.-S., Wang, Q., and Tang, K. Safe delta: Consistently preserving safety when fine-tuning LLMs on diverse datasets. In *Proceedings of Forty-second International Conference on Machine Learning (ICML)*, 2025.
- Meng, F., Du, L., Liu, Z., Zhou, Z., Lu, Q., Fu, D., Shi, B., Wang, W., He, J., Zhang, K., et al. Mm-eureka: Exploring visual aha moment with rule-based large-scale reinforcement learning. *arXiv preprint arXiv:2503.07365*, 2025.
- Noukhovitch, M., Huang, S., Xhonneux, S., Hosseini, A., Agarwal, R., and Courville, A. Faster, more efficient RLHF through off-policy asynchronous learning. In *Proceedings of the Thirteenth International Conference on Learning Representations (ICLR)*, 2025.
- Ouyang, L., Wu, J., Jiang, X., Almeida, D., Wainwright, C., Mishkin, P., Zhang, C., Agarwal, S., Slama, K., Ray, A., et al. Training language models to follow instructions with human feedback. In *Proceedings of Advances in Neural Information Processing Systems (NeurIPS)*, 2022.
- Paul, M., Ganguli, S., and Dziugaite, G. K. Deep learning on a data diet: Finding important examples early in training. In *Proceedings of Advances in Neural Information Processing Systems (NeurIPS)*, 2021.
- Rafailov, R., Sharma, A., Mitchell, E., Manning, C. D., Ermon, S., and Finn, C. Direct preference optimization: Your language model is secretly a reward model. In *Proceedings of Advances in Neural Information Processing Systems (NeurIPS)*, 2023.
- Schulman, J., Wolski, F., Dhariwal, P., Radford, A., and Klimov, O. Proximal policy optimization algorithms. *arXiv preprint arXiv:1707.06347*, 2017.

- Shao, Z., Wang, P., Zhu, Q., Xu, R., Song, J., Bi, X., Zhang, H., Zhang, M., Li, Y., Wu, Y., et al. Deepseekmath: Pushing the limits of mathematical reasoning in open language models. *arXiv preprint arXiv:2402.03300*, 2024.
- Shen, Q., Chen, D., Huang, Y., Ling, Z., Li, Y., Ding, B., and Zhou, J. Bots: A unified framework for bayesian online task selection in llm reinforcement finetuning. *arXiv preprint arXiv:2510.26374*, 2025.
- Sheng, G., Zhang, C., Ye, Z., Wu, X., Zhang, W., Zhang, R., Peng, Y., Lin, H., and Wu, C. Hybridflow: A flexible and efficient rlhf framework. In *Proceedings of the Twentieth European Conference on Computer Systems (EuroSys)*, 2025a.
- Sheng, G., Zhang, C., Ye, Z., Wu, X., Zhang, W., Zhang, R., Peng, Y., Lin, H., and Wu, C. Hybridflow: A flexible and efficient rlhf framework. In *Proceedings of the Twentieth European Conference on Computer Systems (EuroSys)*, 2025b.
- Shi, T., Wu, Y., Song, L., Zhou, T., and Zhao, J. Efficient reinforcement finetuning via adaptive curriculum learning. *arXiv preprint arXiv:2504.05520*, 2025.
- Singhal, P., Goyal, T., Xu, J., and Durrett, G. A long way to go: Investigating length correlations in RLHF. In *Proceedings of First Conference on Language Modeling (COLM)*, 2024.
- Sun, Y., Guo, J., Kok, S., Wang, Z., Wen, Z., and Zhang, Z. Efficient reinforcement learning for large language models with intrinsic exploration. *arXiv preprint arXiv:2511.00794*, 2025a.
- Sun, Y., Shen, J., Wang, Y., Chen, T., Wang, Z., Zhou, M., and Zhang, H. Improving data efficiency for llm reinforcement fine-tuning through difficulty-targeted online data selection and rollout replay. In *Proceedings of Advances in Neural Information Processing Systems (NeurIPS)*, 2025b.
- Sun, Y., Shen, J., Wang, Y., Chen, T., Wang, Z., Zhou, M., and Zhang, H. Improving data efficiency for llm reinforcement fine-tuning through difficulty-targeted online data selection and rollout replay. *arXiv preprint arXiv:2506.05316*, 2025c.
- Tang, X., Zhang, Z., Liu, Y., Zhao, W. X., Wen, Z., Zhang, Z., and Zhou, J. Towards high data efficiency in reinforcement learning with verifiable reward. *arXiv preprint arXiv:2509.01321*, 2025.
- Team, Q. Qwen2.5: A party of foundation models, September 2024. URL <https://qwenlm.github.io/blog/qwen2.5/>.
- Tomihari, A. Learning dynamics in rl post-training for language models. *arXiv preprint arXiv:2601.04670*, 2026.
- Wang, K., Zhang, G., Zhou, Z., Wu, J., et al. A comprehensive survey in llm(-agent) full stack safety: Data, training and deployment. *arXiv preprint arXiv:2504.15585*, 2025a.
- Wang, Y., Yang, Q., Zeng, Z., Ren, L., Liu, L., Peng, B., Cheng, H., He, X., Wang, K., Gao, J., Chen, W., Wang, S., Du, S. S., and Shen, Y. Reinforcement learning for reasoning in large language models with one training example. *arXiv preprint arXiv:2504.20571*, 2025b.
- Wu, J., Fan, W., Chen, J., Liu, S., Li, Q., and Tang, K. Disentangled contrastive learning for social recommendation. In *Proceedings of the 31st ACM International Conference on Information & Knowledge Management (CIKM)*, 2022.
- Wu, J., Fan, W., Chen, J., Liu, S., Liu, Q., He, R., Li, Q., and Tang, K. Condensing pre-augmented recommendation data via lightweight policy gradient estimation. *IEEE Transactions on Knowledge and Data Engineering*, 2025a.
- Wu, J., Liu, Q., Hu, H., Fan, W., Liu, S., Li, Q., Wu, X.-M., and Tang, K. Leveraging chatgpt to empower training-free dataset condensation for content-based recommendation. In *Companion Proceedings of the ACM on Web Conference 2025*, 2025b.
- Xu, Y. E., Savani, Y., Fang, F., and Kolter, J. Z. Not all rollouts are useful: Down-sampling rollouts in llm reinforcement learning. *arXiv preprint arXiv:2504.13818*, 2025.
- Yang, A., Zhang, B., Hui, B., Gao, B., Yu, B., Li, C., Liu, D., et al. Qwen2.5-math technical report: Toward mathematical expert model via self-improvement. *arXiv preprint arXiv:2409.12122*, 2024.
- Yang, A., Li, A., Yang, B., Zhang, B., Hui, B., Zheng, B., et al. Qwen3 technical report. *arXiv preprint arXiv:2505.09388*, 2025.
- Ye, C., Yu, Z., Zhang, Z., Chen, H., Sadagopan, N., Huang, J., Zhang, T., and Beniwal, A. Beyond correctness: Harmonizing process and outcome rewards through rl training. *arXiv preprint arXiv:2509.03403*, 2025a.
- Ye, Y., Huang, Z., Xiao, Y., Chern, E., Xia, S., and Liu, P. LIMO: Less is more for reasoning. In *Proceedings of the Second Conference on Language Modeling (COLM)*, 2025b.
- Yu, Q., Zhang, Z., Zhu, R., Yuan, Y., Zuo, X., Yue, Y., Dai, W., Fan, T., Liu, G., Liu, L., et al. Dapo: An open-source

- llm reinforcement learning system at scale. *arXiv preprint arXiv:2503.14476*, 2025.
- Yuan, Y., Yue, Y., Zhu, R., Fan, T., and Yan, L. What’s behind ppo’s collapse in long-cot? value optimization holds the secret. *arXiv preprint arXiv:2503.01491*, 2025.
- Yue, Y., Yuan, Y., Yu, Q., Zuo, X., Zhu, R., Xu, W., Chen, J., Wang, C., Fan, T., Du, Z., et al. Vapo: Efficient and reliable reinforcement learning for advanced reasoning tasks. *arXiv preprint arXiv:2504.05118*, 2025.
- Zeng, Y., Sun, Z., Ji, B., Min, E., Cai, H., Wang, S., Yin, D., Zhang, H., Chen, X., and Wang, J. Cures: From gradient analysis to efficient curriculum learning for reasoning llms. *arXiv preprint arXiv:2510.01037*, 2025.
- Zhang, E., Yan, X., Lin, W., Zhang, T., and Qianchun, L. Learning like humans: Advancing llm reasoning capabilities via adaptive difficulty curriculum learning and expert-guided self-reformulation. In *Proceedings of the 2025 Conference on Empirical Methods in Natural Language Processing (EMNLP)*, 2025a.
- Zhang, H., Fu, J., Zhang, J., Fu, K., Wang, Q., Zhang, F., and Zhou, G. Rlep: Reinforcement learning with experience replay for llm reasoning. *arXiv preprint arXiv:2507.07451*, 2025b.
- Zhang, X., Li, C., Zong, Y., Ying, Z., He, L., and Qiu, X. Evaluating the performance of large language models on gaokao benchmark, 2023.
- Zhang, X., Wang, J., Cheng, Z., Zhuang, W., Lin, Z., Zhang, M., Wang, S., Cui, Y., Wang, C., Peng, J., Jiang, S., Kuang, S., Yin, S., Wen, C., Zhang, H., Chen, B., and Yu, B. Srpo: A cross-domain implementation of large-scale reinforcement learning on llm. *arXiv preprint arXiv:2504.14286*, 2025c.
- Zhao, Y., Gu, A., Varma, R., Luo, L., Huang, C.-C., Xu, M., Wright, L., Shojanazeri, H., Ott, M., Shleifer, S., et al. Pytorch fsdp: experiences on scaling fully sharded data parallel. *arXiv preprint arXiv:2304.11277*, 2023.
- Zheng, C., Liu, S., Li, M., Chen, X.-H., Yu, B., Gao, C., Dang, K., Liu, Y., Men, R., Yang, A., et al. Group sequence policy optimization. *arXiv preprint arXiv:2507.18071*, 2025a.
- Zheng, H., Zhou, Y., Bartoldson, B. R., Kailkhura, B., Lai, F., Zhao, J., and Chen, B. Act only when it pays: Efficient reinforcement learning for llm reasoning via selective rollouts. *arXiv preprint arXiv:2506.02177*, 2025b.
- Zhou, C., Liu, P., Xu, P., Iyer, S., Sun, J., Mao, Y., Ma, X., Efrat, A., Yu, P., Yu, L., et al. Lima: Less is more for alignment. In *Proceedings of Advances in Neural Information Processing Systems (NeurIPS)*, 2023.

---

# Appendix of HIVE: Online-Verified Prompt Selection for Efficient RL Training of Large Reasoning Model

---

In this appendix, we provide proofs for Theorem 3.1 (Appendix A), the details for experimental settings (Appendix B), detailed related work (Appendix C), additional experiments (Appendix D), and algorithm (Appendix E).

## A. Proof of Theorem 3.1

In this section, we provide a rigorous theoretical analysis of our method. We aim to establish a probabilistic guarantee that the ranking of the prompt-side entropy  $V(x)$  consistently reflects the ranking of the true response-side entropy  $U^*(x)$ .

### A.1. Preliminaries and Notations

Let the fixed model parameters be  $\hat{\theta}$  and the vocabulary size be  $|\mathcal{V}|$ . We denote the sampling policy used for generation as  $q(\cdot|x)$  (e.g., temperature sampling with parameter  $\tau$ ).

**Observable: Prompt-side Entropy.** Given a prompt sequence  $x = (x_1, \dots, x_L)$ , the model computes the probability distribution over the vocabulary at each position. Let  $p_{\hat{\theta}, \tau}(\cdot|x_{<l}) = \text{softmax}(z_{\hat{\theta}}(x_{<l})/\tau)$  denote the temperature-scaled probability. The observable token entropy at position  $l$  is  $e_l(x) := \mathcal{H}(p_{\hat{\theta}, \tau}(\cdot|x_{<l}))$ . We define the aggregated prompt entropy as:

$$V(x) := \frac{1}{L-1} \sum_{l=2}^L e_l(x). \quad (15)$$

**Observable: Response-side Entropy.** For a given prompt  $x$ , we generate  $G$  independent rollouts to estimate the output entropy. For the  $r$ -th rollout, let the response be  $y_{1:L_r}^{(r)}$ . Define the step context as  $c_t^{(r)} := (x, y_{<t}^{(r)})$ . The token entropy at step  $t$  is  $u_t^{(r)}(x) := \mathcal{H}(p_{\hat{\theta}, \tau}(\cdot|c_t^{(r)}))$ . The length-normalized entropy for rollout  $r$  is  $U^{(r)}(x) := \frac{1}{L_r} \sum_{t=1}^{L_r} u_t^{(r)}(x)$ . The final empirical estimator is the average over  $n$  rollouts:

$$\hat{U}(x) := \frac{1}{n} \sum_{r=1}^n U^{(r)}(x). \quad (16)$$

We define the target  $U^*(x) := \mathbb{E}_{y \sim q(\cdot|x)}[U^{(r)}(x)]$  as the expected entropy under the sampling policy.

### A.2. Theoretical Bridges and Assumptions

To bridge the gap between the computationally tractable token-level logits entropy and the model’s high-level semantic entropy, we establish our theoretical analysis upon two pivotal assumptions. First, we map the observable token entropy to the model’s internal representation entropy (*Representation Approximation*). Second, we posit that this internal entropy propagates linearly from the prompt to the response (*Entropy Propagation*).

#### A.2.1. FROM TOKEN TO REPRESENTATION.

While observable entropies  $V(x)$  and  $U^*(x)$  are derived from the final output layer, true epistemic entropy is often better encoded in the latent space. Following (Gao et al., 2025a), we define the *Representation Entropy*  $s(c)$  as the entropy of hidden states at a deep layer  $b \approx N$ , formally  $s(c) \approx \hat{\mathcal{H}}[H^{(b)}|c]$ . We define the aggregated representation entropies for the prompt and response as:

$$S_{\text{prompt}}(x) := \frac{1}{L-1} \sum_{l=2}^L s(x_{<l}), \quad S_{\text{resp}}(x) := \mathbb{E}_y \left[ \frac{1}{T} \sum_{t=1}^T s(c_t) \right]. \quad (17)$$

Based on this definition, we introduce our first assumption to link observables to internal states.

**Assumption A.1** (Representation Approximation). The observable token entropy approximates the internal representation entropy up to a small residual  $\delta$ :

$$|V(x) - S_{\text{prompt}}(x)| \leq \delta \quad \text{and} \quad |U^*(x) - S_{\text{resp}}(x)| \leq \delta. \quad (18)$$

*Justification (Theoretical):* This assumption is grounded in Proposition 1 of (Gao et al., 2025a), which proves that for trained LLMs, the entropy of hidden states in deep layers serves as an approximate upper bound for the predictive posterior entropy (i.e., our token entropy). As the layer depth  $b \rightarrow N$ , the mutual information is maximized, ensuring the token entropy is tightly correlated with the internal representation.

### A.2.2. ENTROPY PROPAGATION.

Having established the link to internal representations, we next model how this entropy evolves from the input context to the generation phase.

**Assumption A.2** (Entropy Propagation). The representation entropy in the prompt propagates linearly to the response generation stage. There exist constants  $a > 0, b \in \mathbb{R}$  such that:

$$|S_{\text{resp}}(x) - (aS_{\text{prompt}}(x) + b)| \leq \epsilon. \quad (19)$$

*Justification (Empirical):* To validate this linearity and quantify the noise  $\epsilon$ , we analyzed 2,048 prompts. We computed  $V(x)$  as the proxy for  $S_{\text{prompt}}$  (per Assumption A.1). To mitigate the intrinsic stochasticity of LLM generation and reveal the underlying propagation law, we employ a binned analysis. As shown in Figure 9, we observe an exceptionally strong positive correlation (Pearson  $r=0.9600$ ) between the prompt and response entropy. By analyzing the data through binned means (blue error bars), we find that the average response entropy scales strictly linearly with prompt entropy. The linear regression fit achieves a high coefficient of determination ( $R^2 = 0.9216$ ), empirically confirming that higher entropy in the prompt representation propagates predictably to the generation phase ( $a > 0$ ), validating the linear structure of Assumption A.2 despite intrinsic generation stochasticity.

### A.3. Concentration Bound

**Lemma A.3** (High-probability Concentration). For any fixed prompt  $x$  and tolerance  $\eta > 0$ , the empirical entropy  $\hat{U}(x)$  concentrates around the true expectation  $U^*(x)$ :

$$\Pr \left( |\hat{U}(x) - U^*(x)| > \eta \right) \leq 2 \exp \left( -\frac{2n\eta^2}{(\log |\mathcal{V}|)^2} \right). \quad (20)$$

Consequently, for any confidence level  $1 - \alpha$  (where  $\alpha \in (0, 1)$ ), with probability at least  $1 - \alpha$ :

$$|\hat{U}(x) - U^*(x)| \leq \eta(\alpha) := \log |\mathcal{V}| \sqrt{\frac{\log(2/\alpha)}{2n}}. \quad (21)$$

*Proof.* The sequence-level entropy  $U^{(r)}(x)$  for each rollout is bounded within  $[0, \log |\mathcal{V}|]$ . Since the  $n$  rollouts are generated independent and identically distributed (i.i.d.) from the sampling policy  $q(\cdot|x)$ , Hoeffding’s inequality (Hoeffding, 1963) applies directly to the empirical mean  $\hat{U}(x)$ , yielding the stated bound.  $\square$

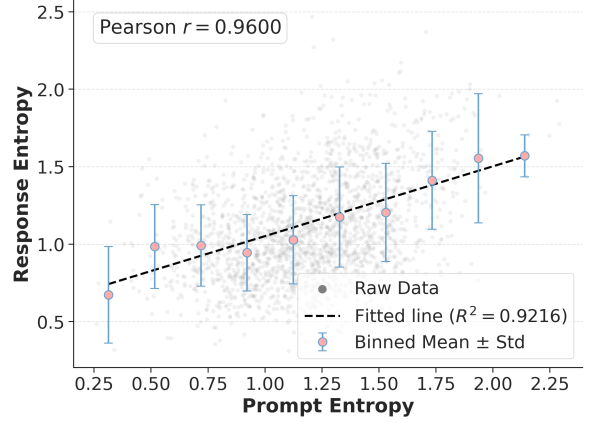


**Figure 9. Validation of Entropy Propagation (Assumption A.2).** The scatter plot illustrates the relationship between Prompt Mean Entropy and Response Entropy over 2,048 samples. Due to the stochastic nature of generation, we visualize binned statistics (blue points, mean  $\pm$  std) to disentangle the linear signal from individual sample noise (grey dots). The regression line on the binned data exhibits an exceptional fit ( $R^2 = 0.9216, r = 0.9600$ ), confirming that prompt entropy linearly dictates the expected response entropy.

#### A.4. Main Result: Rank Consistency

**Theorem A.4** (Theorem 3.1). *Consider a pair of prompts  $(x, x')$ . Let  $\Delta_V := V(x) - V(x')$  be the observable difference in prompt entropy, and  $\Delta_U := \hat{U}(x) - \hat{U}(x')$  be the difference in estimated response entropy. Under Assumptions A.1 and A.2, for any  $\alpha \in (0, 1)$ , with probability at least  $1 - 2\alpha$ :*

$$|\Delta_U - a\Delta_V| \leq 2\epsilon + 2(a+1)\delta + 2\eta(\alpha). \quad (22)$$

Crucially, if the prompt entropy margin satisfies  $|a\Delta_V| > 2\epsilon + 2(a+1)\delta + 2\eta(\alpha)$ , then the ranking is preserved:

$$\text{sign}(\hat{U}(x) - \hat{U}(x')) = \text{sign}(V(x) - V(x')). \quad (23)$$

*Proof.* We decompose the error into three components: sampling noise, propagation residual, and representation approximation error.

**Step 1: Sampling Noise.** By applying Lemma A.3 and a union bound over prompts  $x$  and  $x'$ , with probability  $\geq 1 - 2\alpha$ , the empirical estimates are close to their true expectations:

$$|\Delta_U - (U^*(x) - U^*(x'))| \leq 2\eta(\alpha). \quad (24)$$

**Step 2: Propagation Dynamics.** From Assumption A.2, we express the response representation entropy as  $S_{\text{resp}}(x) = aS_{\text{prompt}}(x) + b + \xi(x)$  where  $|\xi(x)| \leq \epsilon$ . The difference between two prompts cancels out the bias term  $b$ :

$$|(S_{\text{resp}}(x) - S_{\text{resp}}(x')) - a(S_{\text{prompt}}(x) - S_{\text{prompt}}(x'))| \leq 2\epsilon. \quad (25)$$

**Step 3: Representation Approximation.** Using Assumption A.1, we substitute the theoretical representation entropies with observable token entropies. We have  $|(U^*(x) - U^*(x')) - (S_{\text{resp}}(x) - S_{\text{resp}}(x'))| \leq 2\delta$  and  $|(S_{\text{prompt}}(x) - S_{\text{prompt}}(x')) - \Delta_V| \leq 2\delta$ . Applying the triangle inequality and scaling the prompt-side error by  $a$ :

$$|(U^*(x) - U^*(x')) - a\Delta_V| \leq 2\epsilon + 2\delta + 2a\delta = 2\epsilon + 2(a+1)\delta. \quad (26)$$

Combining Eq. (24) and Eq. (26) yields the final bound in Eq. (22). The condition  $|a\Delta_V| > \text{RHS}$  (Right-Hand Side) ensures that the signal magnitude exceeds the worst-case cumulative noise, guaranteeing that the sign of the difference remains unchanged.  $\square$

## B. Detailed Experimental Setting for Main Study

For the experimental settings, we mainly follow GRESO (Zheng et al., 2025b). The details are introduced as follows.

**Models & Datasets.** We run our experiments on Qwen2.5-Math-1.5B (Yang et al., 2024), DeepSeek-R1-Distill-Qwen-1.5B (Guo et al., 2025), Qwen2.5-Math-7B (Yang et al., 2024), and Llama-3.2-3B-Instruct (Grattafiori et al., 2024). For Qwen2.5-Math-1.5B/7B, we set the context length to 4096. For DeepSeek-R1-Distill-Qwen-1.5B and Llama-3.2-3B-Instruct, we set the context length to 8196. For training datasets, we evaluate our methods with two datasets following (Zheng et al., 2025b): 1) DAPO+MATH (DM): It is the combination of DAPO dataset (Yu et al., 2025) and MATH dataset (Hendrycks et al., 2021), which also contains LaTeX-formatted solutions. 2) OPEN-R1 30k subset (R1): 30,000-example subset of the OPEN-R1 math dataset (Hugging Face, 2025).

**Training & Evaluation.** Our method is implemented based on verl (Sheng et al., 2025b) and vLLM (Kwon et al., 2023). We use  $8 \times A100$  GPUs for all experiments. We follow GRESO (Zheng et al., 2025b) to set the rollout sampling temperature to 1. For Qwen2.5-Math-1.5B/7B and Llama-3.2-3B-Instruct, the training batch size is set to 256, rollout sampling batch size to 384, and the mini-batch size to 512. For DeepSeek-R1-Distill-Qwen-1.5B, the training batch size is set to 128, the rollout sampling batch size to 192, and the mini-batch size to 512. We sample 8 responses per prompt. For all four models, we use  $8 \times A100$  for training. For DeepSeek-R1-Distill-Qwen-1.5B and Llama-3.2-3B-Instruct, we set the context length to 8196. For Qwen2.5-Math-1.5B/7B, we set the context length to 4096. All the models are trained for 1000 steps, and the optimizer is AdamW (Loshchilov & Hutter, 2019) with a constant learning rate of  $1e-6$ ,  $\beta_1 = 0.9$ ,  $\beta_2 = 0.999$ , and a weight decay of 0.01. We use the following question template to prompt the LLM. For reward assignment, we give a score of 0.1 for

successfully extracting an answer and a score of 1.0 if the extracted answer is correct. Similar to (Yu et al., 2025), we remove the KL-divergence term. The optimization is performed on the parameters of the actor module wrapped with Fully Sharded Data Parallel (FSDP) (Zhao et al., 2023) for efficient distributed training. For benchmark datasets, we use six widely used complex mathematical reasoning benchmarks to evaluate the performance of trained models: Math500 (Hendrycks et al., 2021), AIME24 (Art of Problem Solving, 2024a), AMC (Art of Problem Solving, 2024b), Minerva Math (Lewkowycz et al., 2022), Gaokao (Zhang et al., 2023), and Olympiad Bench (He et al., 2024). Following (Zheng et al., 2025b), we evaluate models on those benchmarks every 50 steps and report the performance of the checkpoint that obtains the best average performance on six benchmarks.

#### Question Template

Please solve the following math problem: {{Question Description}}. The assistant first thinks about the reasoning process step by step and then provides the user with the answer. Return the final answer in `\boxed{}` tags, for example `\boxed{1}`. Let’s solve this step by step.

### C. Detailed Related Work

**RL for LLM Reasoning.** Reinforcement learning (RL) has become a key technique for post-training large language models (LLMs) (Christiano et al., 2017; Bai et al., 2022). Early work (Ouyang et al., 2022; Rafailov et al., 2023) used RL to incorporate reward signals from human feedback, enabling LLMs to generate faithful and harmless responses that follow instructions and align with human preferences. More recently, reinforcement learning with verifiable rewards (RLVR) has emerged as a strong alternative (Guo et al., 2025; Hu, 2025; Liu et al., 2025; Jaech et al., 2024; Zhang et al., 2025c; Wang et al., 2025a). Instead of relying on a learned reward model, RLVR optimizes policies using verifiable reward signals. This leads to large gains in reasoning, especially in mathematics and programming. Building on RLVR, subsequent work has developed RL algorithms tailored to LLM reasoning, most commonly within the Proximal Policy Optimization (PPO) (Schulman et al., 2017) and Generalized Relative Policy Optimization (GRPO) (Shao et al., 2024) frameworks. For example, VC-PPO (Yuan et al., 2025) and VAPO (Yue et al., 2025) improve reasoning by strengthening value-function learning under PPO. In contrast, RLOO (Ahmadian et al., 2024) and GRPO (Shao et al., 2024) use multi-sample baselines to avoid explicit value learning, enabling efficient and stable updates. Some studies (Liang et al., 2025; Li et al., 2025a; Zhang et al., 2025b; Lu et al., 2025) also explore experience-replay variants that incorporate historical trajectories or expert demonstrations to enhance LLM reasoning. Other work modifies the optimization objective to improve stability and reduce bias (Liu et al., 2025; Chu et al., 2025; Huang et al., 2025): Dr. GRPO (Liu et al., 2025) analyzes and mitigates systematic optimization bias during training, while GSPO (Zheng et al., 2025a) replaces token-level ratio/clipping with sequence-level counterparts. However, these methods still under-explore rollouts at the frontier of model capability. DAPO (Yu et al., 2025) further improves sample efficiency by filtering instances that are consistently correct or consistently incorrect across multiple rollouts, but it relies on costly multi-sample evaluation to identify such instances, which limits scalability.

**Data Efficient LLM Training.** Data quality and selection are key drivers of LLM performance. Consistent with the “less is more” principle, small curated datasets can match or outperform finetuning on large noisy corpora in SFT (Zhou et al., 2023; Ye et al., 2025b), and reinforced finetuning similarly depends on prompt and trajectory quality—making data curation central to efficient learning. A common approach is offline filtering, which ranks prompts before finetuning using static heuristics (e.g., difficulty, domain balance, diversity) (Wang et al., 2025b; Fatemi et al., 2025; Li et al., 2025b; Shi et al., 2025; Tang et al., 2025; Wu et al., 2025a; 2022). However, it adds substantial preprocessing cost and cannot adapt to the model’s rapidly changing competence during training. To address this, recent work explores online selection, dynamically choosing prompts conditioned on the current policy. A line of work adopts step-wise selection: at each training step, it rollouts and evaluate candidate prompts to discard uninformative prompts (Yu et al., 2025; Meng et al., 2025; Foster et al., 2025; Xu et al., 2025; Lin et al., 2025; Sun et al., 2025a; Wu et al., 2025b) or prioritize those of medium difficulty (Bae et al., 2025), but these methods requires repeated rollouts and evaluations, incurring substantial computational overhead. Other methods evaluate without direct rollout by maintaining historical logs and applying heuristics (Zheng et al., 2025b) or Bayesian estimators (Chen et al., 2025b; Zeng et al., 2025; Shen et al., 2025) to filter prompts; however, they introduce additional memory overhead and can suffer from large estimation errors. In contrast, some studies use auxiliary model to estimate difficulty. For example, DOTS (Sun et al., 2025c) trains an auxiliary model and rollouts a small set of reference tasks to infer the difficulty of the remaining prompts, whereas PCL (Gao et al., 2025c) leverages an on-policy value model updated jointly with the policy to identify medium-difficulty prompts; however, these methods impose non-trivial additional compute

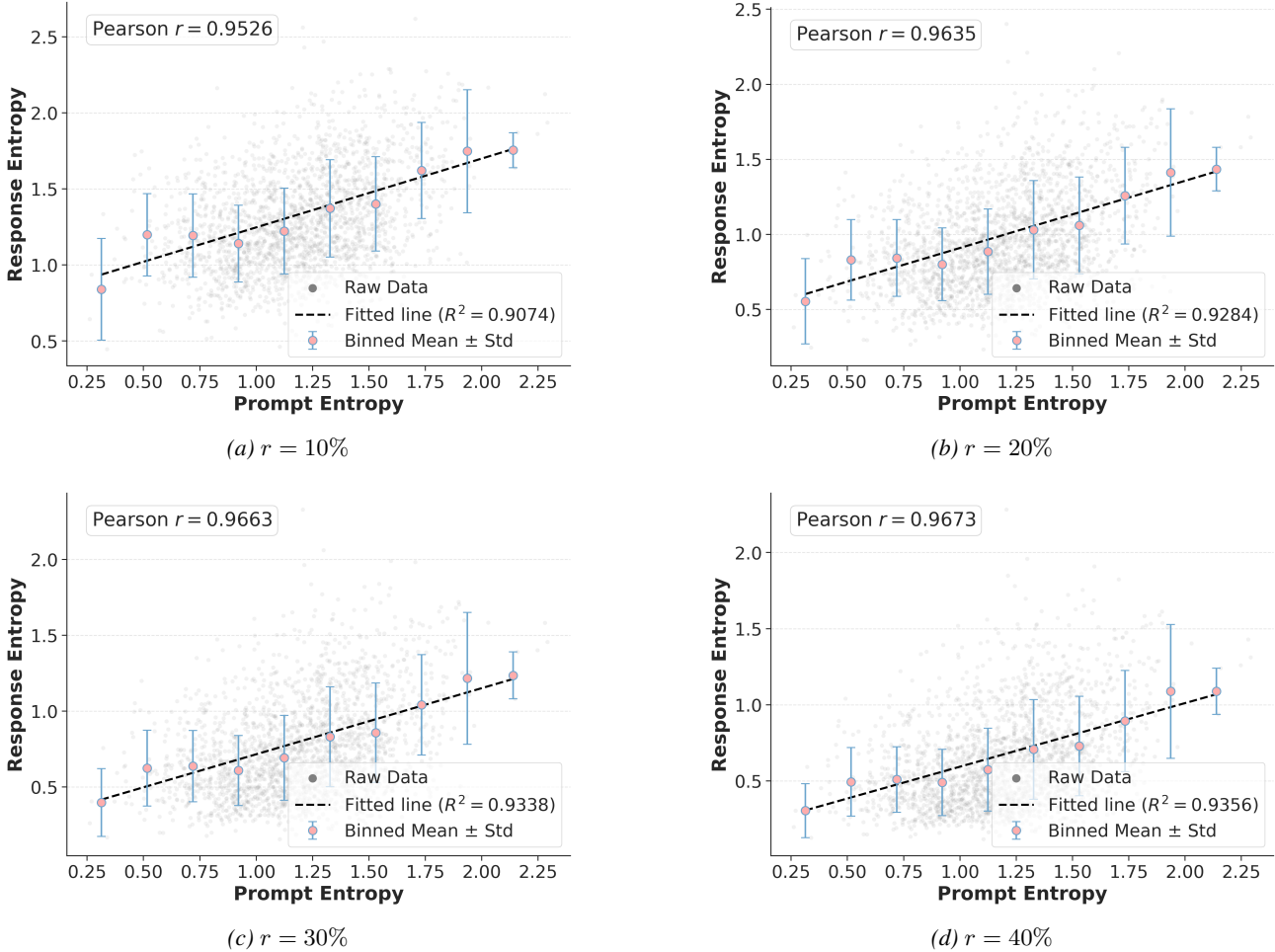


Figure 10. Relationship between prompt entropy and response entropy computed over the top- $r\%$  tokens in the response distribution, sweeping  $r \in \{10, 20, 30, 40\}$ . Each panel reports the binned mean trend under the corresponding ratio setting.

and memory costs for policy optimization. Another approaches adopt stage-wise data curation periodically re-estimates difficulty to refresh the training set (Zhang et al., 2025a;c), but it is often insufficiently adaptive and fails to track real-time learning dynamics.

In contrast, our method, HIVE, establishes a hierarchical filtering paradigm that simultaneously achieves the high precision of online selection and the low overhead of historical heuristics. Unlike rollout-dependent approaches (Yu et al., 2025; Xu et al., 2025) that incur prohibitive costs by generating full responses before filtering, HIVE leverages prompt entropy as a cost-effective proxy to preemptively prune uninformative samples. Furthermore, distinct from estimator-based methods (Zheng et al., 2025b) that suffer from metadata staleness as the model updates, HIVE employs this real-time verification to dynamically track the shifting “learning edge.” This allows HIVE to discard prompts that have become trivial or intractable in the current iteration, eliminating the resource waste caused by the discrepancy between historical logs and real-time capability. By integrating history-informed priors with online-verified precision, HIVE offers a Pareto-optimal solution for scaling RLVR efficiently.

## D. Additional Experiments

### D.1. Correlation Between Prompt Entropy and Response Entropy

Building on the empirical validation of Assumption A.2, we conduct an additional robustness study by redefining the response entropy  $S_{\text{resp}}(x)$  as the entropy computed over only the top- $r\%$  tokens of the response distribution, sweeping

$r \in \{10, 20, 30, 40\}$ . To suppress intrinsic decoding stochasticity, we follow the same binned-mean protocol on 2,048 prompts, binning by  $S_{\text{prompt}}(x)$  (proxied by  $V(x)$ ) and averaging  $S_{\text{resp}}^{(r)}(x)$  within each bin. As shown in Figure 10, the prompt–response relationship remains strongly linear across all ratios. This indicates that the observed entropy propagation law is a stable property of the generation dynamics, further strengthening the linear structure and bounded-noise characterization in Assumption A.2.

## D.2. Case Study

To gain deeper insight into the behavior of our selective filtering algorithm, we analyze a case study based on prompts from the MATH dataset. We divide these prompts into four categories: Frequently Skipped Prompts (Easy), Frequently Skipped Prompts (Hard), Frequently Selected Prompts, and Prompts Frequently Selected by Stage 1 but Skipped by Stage 2. We observe that frequently skipped easy prompts often involve simple computations or routine use of formulas, leading to high solution rates across sampled responses. In contrast, hard prompts that are often skipped tend to be too difficult for the model, leading to low or zero success across rollouts, limiting their value for training. Frequently selected prompts tend to be moderately difficult, making consistent contributions to model learning. Furthermore, we analyze the prompts selected in stage 1 but filtered after stage 2. Most prompts are relatively easy, showing that the historical information is not reliable for filtering.

### Frequently Skipped Prompts (Easy)

- Question:** What is the value of  $(2x + 5)^2$  when  $x = 3$ ? **Solution:** 121.
- Question:** Solve for  $x$ :  $5^{x+4} = 125^x$ ? **Solution:** 21.
- Question:** A squirrel travels at a constant 4 miles per hour. How long does it take for this squirrel to travel 1 mile? Express your answer in minutes. **Solution:** 15.
- Question:** Evaluate  $\log_5 625$ . **Solution:** 4.
- Question:** What value of  $x$  will give the minimum value for  $x^2 - 10x + 24$ ? **Solution:** 5.

### Frequently Skipped Prompts (Hard)

- Question:** Let  $\triangle PQR$  be a right triangle with  $PQ = 90$ ,  $PR = 120$ , and  $QR = 150$ . Let  $C_1$  be the inscribed circle. Construct  $\overline{ST}$  with  $S$  on  $\overline{PR}$  and  $T$  on  $\overline{QR}$ , such that  $\overline{ST}$  is perpendicular to  $\overline{PR}$  and tangent to  $C_1$ . Construct  $\overline{UV}$  with  $U$  on  $\overline{PQ}$  and  $V$  on  $\overline{QR}$  such that  $\overline{UV}$  is perpendicular to  $\overline{PQ}$  and tangent to  $C_1$ . Let  $C_2$  be the inscribed circle of  $\triangle RST$  and  $C_3$  the inscribed circle of  $\triangle QUV$ . The distance between the centers of  $C_2$  and  $C_3$  can be written as  $\sqrt{10n}$ . What is  $n$ ? **Solution:** 725.
- Question:** Consider the region  $A$  in the complex plane that consists of all points  $z$  such that both  $\frac{z}{40}$  and  $\frac{40}{z}$  have real and imaginary parts between 0 and 1, inclusive. Find the area of  $A$ . **Solution:**  $1200 - 200\pi$ .
- Question:** Ephram is growing 3 different variants of radishes in a row of 13 radishes total, but he forgot where he planted each radish variant and he can't tell what variant a radish is before he picks it. Ephram knows that he planted at least one of each radish variant, and all radishes of one variant will form a consecutive string, with all such possibilities having an equal chance of occurring. He wants to pick three radishes to bring to the farmers market, and wants them to all be of different variants. Given that he uses optimal strategy, the probability that he achieves this can be expressed as  $\frac{m}{n}$ , where  $m$  and  $n$  are relatively prime positive integers. Find  $m + n$ . **Solution:** 17.
- Question:** There are 1000 rooms in a row along a long corridor. Initially, the first room contains 1000 people, and the remaining rooms are empty. Each minute, the following happens: for each room containing more than one person, someone in that room decides it is too crowded and moves to the next room. All these movements are simultaneous (so nobody moves more than once within a minute). After one hour, how many different rooms will have people in them? **Solution:** 31.
- Question:** A regular hexagon has side length 6. Congruent arcs with radius 3 are drawn with the center at each of the vertices, creating circular sectors as shown. The region inside the hexagon but outside the sectors is shaded as shown. The original answer is in the form  $a\sqrt{b} - c\pi$ . Please find the value of  $a + b + c$ . **Solution:** 75.

Frequently Selected Prompts After Stage 2

1. **Question:** Let  $z$  be a complex number such that

$$|z - 12| + |z - 5i| = 13.$$

Find the smallest possible value of  $|z|$ . **Solution:**  $\frac{60}{13}$ .

2. **Question:** Find all real solutions to  $x^4 + (2 - x)^4 = 34$ . Enter all the solutions, separated by commas. **Solution:**  $1 + \sqrt{2}, 1 - \sqrt{2}$ .

3. **Question:** Let  $b$  be a real number randomly selected from the interval  $[-17, 17]$ . Then,  $m$  and  $n$  are two relatively prime positive integers such that  $mn$  is the probability that the equation  $x^4 + 25b^2 = (4b^2 - 10b)x^2$  has at least two distinct real solutions. Find the value of  $m + n$ . **Solution:** 63.

4. **Question:** Let  $a, b, c, d$  be real numbers such that

$$\frac{(a-b)(c-d)(b-c)(d-a)}{(a-b)(c-d)} = 25.$$

Find the sum of all possible values of

$$\frac{(a-c)(b-d)}{(a-b)(c-d)}.$$

**Solution:**  $-\frac{3}{2}$ .

5. **Question:** The function  $f$ , defined on the set of ordered pairs of positive integers, satisfies the following properties:

$$\begin{aligned} f(x, x) &= x, \\ f(x, y) &= f(y, x), \quad \text{and} \\ (x + y)f(x, y) &= yf(x, x + y). \end{aligned}$$

Calculate  $f(14, 52)$ . **Solution:** 364.

Prompts Frequently Selected by Stage 1 but Skipped by Stage 2

1. **Question:** A polynomial with integer coefficients is of the form

$$9x^4 + a_3x^3 + a_2x^2 + a_1x + 15 = 0.$$

Find the number of different possible rational roots of this polynomial. **Solution:** 16.

2. **Question:** When an integer is divided by 15, the remainder is 7. Find the sum of the remainders when the same integer is divided by 3 and by 5. **Solution:** 3.

3. **Question:** Find the number of positive divisors of 2002. **Solution:** 16.

4. **Question:** What is the base five product of the numbers  $121_5$  and  $11_5$ ? **Solution:** 1331.

5. **Question:** If  $\sin x = 3 \cos x$ , then what is  $\sin x \cos x$  **Solution:**  $\frac{3}{10}$ .

## E. Algorithm

The HIVE training procedure is illustrated in Algorithm 1. The process begins with **History-Informed Selection**, where the system iteratively samples raw prompts from the dataset  $\mathcal{D}$ . For each sampled prompt, we retrieve its historical metadata, consisting of the consecutive zero-variance counts  $z_i$  and the historical response entropy  $H_i$ . These metrics are combined into a selection probability  $P_{select}$  using a weighted combination of reward decay and entropy normalization. We employ Bernoulli sampling to accumulate a candidate pool  $\mathcal{D}_{cand}$  until its size reaches twice the target training batch size (i.e.,  $2 \cdot B_t$ ). This  $2\times$  oversampling strategy is a prerequisite for the subsequent median-based truncation, ensuring the final batch size aligns with the target computational budget.

**Algorithm 1** Training Iteration in HIVE

---

**Require:** Dataset  $\mathcal{D}$ ; Historical trace  $\mathcal{T}$ ; Target training batch size  $B_t$ ; Group size  $G$ ; Base exploration probability  $p_{e,easy}$ ,  $p_{e,hard}$ ; Step size  $\Delta p$ ; Target zero-var ratio  $\alpha$ .

- 1:  $\mathcal{D}_{cand} \leftarrow \emptyset$
- 2:  $n_{easy}, n_{hard}, n_{total} \leftarrow 0, 0, 0$
- 3: *# Stage 1: History-Informed Selection*
- 4: **repeat**
- 5:    $\{x_i\} \leftarrow$  Sample raw prompts from  $\mathcal{D}$
- 6:   **for** each  $x_i$  in batch **do**
- 7:     Retrieve zero-var count  $z_i$  and history entropy  $H_i$  from  $\mathcal{T}$
- 8:      $P_{Rew} \leftarrow p_e^{z_i}$ ;    $P_{Ent} \leftarrow \text{Normalize}(H_i)$
- 9:      $P_{select} \leftarrow \lambda P_{Rew} + (1 - \lambda) P_{Ent}$
- 10:    **if** Bernoulli( $P_{select}$ ) = 1 **then**
- 11:      $\mathcal{D}_{cand} \leftarrow \mathcal{D}_{cand} \cup \{x_i\}$
- 12:    **end if**
- 13:   **end for**
- 14: **until**  $|\mathcal{D}_{cand}| \geq 2 \cdot B_t$
- 15: *# Stage 2: Online-Verified Selection (Deterministic Gate)*
- 16: Calculate prompt entropy  $V(x)$  for all  $x \in \mathcal{D}_{cand}$
- 17:  $\gamma \leftarrow \text{median}(\{V(x) \mid x \in \mathcal{D}_{cand}\})$
- 18:  $\mathcal{D}_{final} \leftarrow \{x \in \mathcal{D}_{cand} \mid V(x) \geq \gamma\}$
- 19: *# Rollout Phase*
- 20:  $\{x_i, r_i\} \leftarrow$  Generate  $G$  rollouts for each  $x \in \mathcal{D}_{final}$
- 21: *# GRPO Training*
- 22: Update policy model  $\pi_\theta$  using GRPO on  $\{x_i, r_i\}$
- 23: *# History Update & Statistics*
- 24: Update  $\mathcal{T}$  with new rewards and response entropies
- 25:  $n_{total} \leftarrow |\mathcal{D}_{final}|$
- 26:  $n_{easy} \leftarrow \text{count\_zero\_var}(\text{easy\_subset})$ ;    $n_{hard} \leftarrow \text{count\_zero\_var}(\text{hard\_subset})$
- 27: *# Adaptive Exploration Adjustment*
- 28: **for** type  $\in \{easy, hard\}$  **do**
- 29:   **if**  $n_{\text{type}}/n_{total} > \alpha$  **then**
- 30:      $p_{e,\text{type}} \leftarrow p_{e,\text{type}} - \Delta p$
- 31:   **else**
- 32:      $p_{e,\text{type}} \leftarrow p_{e,\text{type}} + \Delta p$
- 33:   **end if**
- 34: **end for**

---

Once the candidate pool is populated, the flow transitions to **Online-Verified Selection**, a deterministic gatekeeper grounded in the model’s current state. For every candidate in  $\mathcal{D}_{cand}$ , we compute the prompt-side entropy  $V(x)$  via a single efficient forward pass. To adaptively identify the current learning edge, we calculate the median entropy  $\gamma = \text{median}(\{V(x)\})$  of the accumulated pool. A strict filter is then applied to retain only prompts where  $V(x) \geq \gamma$ . This step effectively discards the bottom 50% of samples with low uncertainty, yielding a final high-utility batch  $\mathcal{D}_{final}$ .

With the filtered batch established, the system proceeds to the normal **Rollout and Policy Update** phase, which is identical to the GRPO algorithm. After training finishes, the resulting rewards and response entropies are immediately written back to the historical trace  $\mathcal{T}$  to update the metadata for future iterations.